Deposition of II-VI Thin Films by LP-MOCVD Using Novel Single-Source Precursors

Mohammad Afzaal,[a] David Crouch,[a] Mohmmad A. Malik,[a] Majid Motevalli,[b] Paul O'Brien,*[a] Jin-Ho Park,[a] and J. Derek Woollins[c]

Keywords: Chemical vapour deposition / Chalcogens / Zinc / Cadmium

Thin films of several zinc or cadmium chalcogenides have been deposited on glass substrates by low pressure metal-organic chemical vapour deposition (LP-MOCVD) using single-source precursors, $[M\{(EP\textit{i}Pr_2)_2N\}_2]$ (M = Cd^{II}, Zn^{II} and E = S, Se). X-ray single crystal structures show that $[Zn\{(EP\textit{i}Pr_2)_2N\}_2]$ (E = S or Se) and $[Zn\{(SePPh_2)_2N\}_2]$ are tetrahedrally distorted. TGA analyses showed that the precursors are volatile, making them suitable for MOCVD studies. As-deposited films were polycrystalline as confirmed by X-ray powder diffraction (XRPD) and their morphologies were studied by scanning electron microscope (SEM).

Introduction

The direct nature of band gaps in II-VI materials makes them suitable for use in devices, such as blue/blue-green laser diodes,[1−3] which could lead to high-density optical storage systems.[4−6] Cadmium chalcogenides are also useful materials in solid-state solar cells, photoconductors, field effect transistors, sensors and tranducers.[7,8]

Single-source precursors have several potential advantages over conventional MOCVD which uses dual-sources. These include limited premature reactions and good quality homogeneous films.[1] The solid-state chemistry of cadmium and zinc with the chalcogens is typified by the formation of polymeric structures with tetrahedral metal ions,[1] the admantyl structures of many thiolates with zinc and cadmium provide well-characterised examples of such behaviour,[2−4] as do the polymeric chain complexes formed by pyridinethione and 2,3-mercaptobenzothiazole with cadmium and zinc.[5,6] Bochmann et al. have extended such chemistry by producing a range of precursors based on 2,4,6-tri-*tert*-butylphenylchalcogenolate, which have been used to deposit thin films of the metal sulfides and selenides in low-pressure growth experiments.[7−9] In related work, Arnold and co-workers have also deposited a range of chalcogenides using silicon-based ligands, i.e. $[\{MESi(SiCH_3)_3\}_2]$ (M = Zn^{II}, Cd^{II}, Hg^{II} and E = S, Se or Te).[10,11]

Other classes of molecules, which have proved useful for the deposition of thin films include coordination complexes such as dialkyl dichalcogenocarbamates or dithiophosphinates.[12−16] Various groups have studied simple $[M(S_2CNEt_2)_2]$ (M = Cd^{II}, Zn^{II}) complexes and deposited CdS or ZnS films by different deposition techniques.[13−15] However, the use of metal diethyldiselenocarbamates to deposit ZnSe and CdSe on glass substrates resulted in the deposition of elemental selenium.[16] Asymmetrical alkyl substituents as in $[M(E_2CNMeHex)_2]$ (M = Cd^{II}, Zn^{II} and E = S, Se) which were originally introduced in order to increase volatility and have been successfully used to deposit II−VI films (including ZnSe and CdSe) by low pressure metal-organic chemical vapour deposition (LP-MOCVD). An investigation into decomposition mechanisms by gas chromatography mass spectroscopy (GC-MS) and electron impact mass spectroscopy (EI-MS) showed that the deposition of selenium during growth is inhibited in such compounds.[16]

We have recently identified a new class of metal-organic single-source precursors based on bis(diphenylphosphanyl-amine) e.g., $[NH(SePPh_2)_2]$ ligands (an analogue of the β-diketonates) a system pioneered by Woollins, $[M\{(SePPh_2)_2N\}_2]$ (M = Cd^{II}, Zn^{II}) complexes which have been used as precursors for zinc/cadmium selenide films by LP-MOCVD.[17] In this paper, we report crystal structures of $[Zn\{(EP\textit{i}Pr_2)_2N\}_2]$ (E = S or Se) and $[Zn\{(SePPh_2)_2N\}_2]$. We also report the deposition and characterisation of metal chalcogenide films on glass substrates from

[a] The Manchester Materials Science Centre and Department of Chemistry, The University of Manchester,
Oxford Road, Manchester, M13 9PL, UK
Fax: (internat.) +44-(0)161-2754616
E-mail: paul.obrien@man.ac.uk
[b] Department of Chemistry, Queen Mary and Westfield College, Mile End Road, London, E1 4NS, UK
[c] School of Chemistry, University of St. Andrews, Purdie Building,
St. Andrews, Fife, KY16 9ST, UK

$[M\{(EP{i}Pr_2)_2N\}_2]$ (M = Cd^{II}, Zn^{II} and E = S, Se) complexes **1**−**4**) by low-pressure MOCVD.

Results and Discussion

The syntheses of ligands $[NH(EP{i}Pr_2)_2]$ (E = S or Se) were carried out according to previously reported methods.[18,19] The synthesis of the precursor involves deprotonation of the N−H moiety, using sodium methoxide, to form anionic chelate complexes which is subsequently reacted with the metal chloride (Scheme 1). These reactions have some advantages over the routes via metal carbonates and higher yields are obtained particularly for the selenium complexes. The reactions occur efficiently and cleanly at room temperature in anhydrous methanol. All the compounds are soluble in organic solvents and are air-stable.

$$NH(SiMe_3)_2 + 2\ {}^{i}Pr_2PCl \xrightarrow[\text{stirring (3 hours)}]{50\text{–}70\ ^{\circ}C} NH(P{}^{i}Pr_2)_2 + 2\ ClSiMe_3 \quad \text{(Eq. 1)}$$

$$NH(SiMe_3)_2 \xrightarrow[\text{reflux}]{E = S,\ Se} NH(EP{}^{i}Pr_2)_2 \quad \text{(Eq. 2)}$$

$$2\ NH(EP{}^{i}Pr_2)_2 + MCl_2 \xrightarrow[MeOH]{NaOMe} M[(EP{}^{i}Pr_2)_2N]_2 + 2\ NaCl \quad \text{(Eq. 3)}$$

Scheme 1

X-ray Structures

Crystals of $[Zn\{(SePPh_2)_2N\}_2]$ suitable for X-ray diffraction studies were obtained by slow diffusion of hexane into a chloroform solution of the complex. During attempts to synthesise the mixed-alkylzinc complexes by comproportionation reactions between dimetylzinc and $[Zn\{(EP{i}Pr_2)_2N\}_2]$ (E = S or Se), the serendipitous formation of $[Zn\{(EP{i}Pr_2)_2N\}_2]$ (E = S or Se) crystals from toluene solutions occurred. The molecular structures of the compounds are shown in Figures 1−3.

X-ray single crystallographic studies carried out on $[Zn\{(EP{i}Pr_2)_2N\}_2]$ (E = S or Se) and $[Zn\{(SePPh_2)_2N\}_2]$ reveal that the complexes are tetrahedrally coordinated by two ligands. The structure of $[Zn\{(SeP{i}Pr_2)_2N\}_2]$ illustrated in Figure 1 is isostructural with its sulfur analogue (Figure 2). The Zn−Se bond lengths are in the range of 2.458(9) to 2.467(9) Å which are slightly larger than Zn−S bond lengths [2.350(11) to 2.359(11) Å]. Similarly, the Se−Zn−Se bite angles are also increased from the bite angles of S−Zn−S [111.84(4)−112.81(4)°] (Tables 2 and 3). Shortening of the P−N bonds to 1.583(3)−1.592(4) Å and

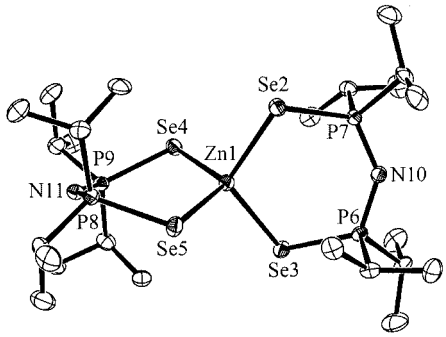

Figure 1. X-ray single crystal structure of $[Zn\{(SeP{i}Pr_2)_2N\}_2]$

Table 1. Crystallographic data collection and refinement parameters

Compound	$C_{24}H_{56}N_2P_4Se_4Zn$	$C_{24}H_{56}N_2P_4S_4Zn$	$C_{48}H_{40}N_2P_4Se_4Zn$
Formula mass	877.70	690.20	1149.91
Temperature (K)	160(2)	160(2)	433(2)
Crystal size (mm)	0.45 × 0.13 × 0.10	0.4 × 0.3 × 0.2	0.57 × 0.45 × 0.35
Crystal system	triclinic	triclinic	triclinic
Space group	$P\bar{1}$	$P\bar{1}$	$P\bar{1}$
a (Å)	9.348(2)	9.232(3)	13.727(7)
b (Å)	12.880(3)	12.678(4)	13.809(5)
c (Å)	16.389(4)	16.401(5)	14.3120(16)
α (°)	100.95(2)	92.24(2)	82.74(9)
β (°)	102.02(2)	101.77(2)	66.36(6)
γ (°)	69.64(2)	110.77(2)	70.13(4)
V (Å^3)	1794.5(7)	1744.1(10)	2337.2(15)
Z	2	2	2
$d_{calcd.}$ (mg/m^3)	1.625	1.314	1.634
Abs. coeff. (mm^{-1})	4.936	1.144	3.813
F(000)	880	736	1136
Index ranges	$0 \le h \le 11$	$-1 \le h \le 5$	$-14 \le h \le 16$
	$-14 \le k \le 15$	$-15 \le k \le 14$	$-16 \le k \le 16$
	$-19 \le l \le 19$	$-19 \le l \le 19$	$-16 \le l \le 16$
Collected/unique	6877/6313	4697/4101	8661/8661
Data/restraints/pars.	6313/0/332	4191/0/332	8661/0/4392
Goodness-of-fit on F^2	0.873	0.895	0.982
$R1$, $wR2$ [$I > 2\sigma(I)$]	0.0297, 0.0745	0.0270, 0.0662	0.0596, 0.1763
$R1$, $wR2$ (all data)	0.0592, 0.0866	0.0365, 0.0706	0.0787, 0.1963
Diff. peak, hole (e·Å^{-3})	0.545, −0.482	0.340, −0.503	1.939, −3.706

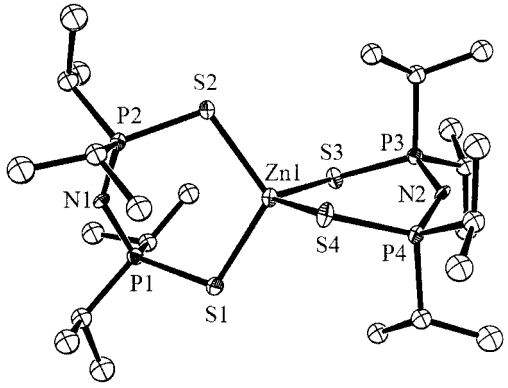

Figure 2. X-ray single crystal structure of $[Zn\{(SPiPr_2)_2N\}_2]$

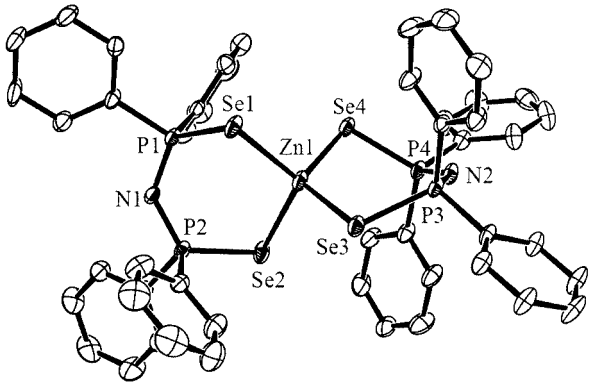

Figure 3. X-ray single crystal structure of $[Zn\{(SePPh_2)_2N\}_2]$

Table 2. Selected interatomic distances (Å) and angles (°) for $[Zn\{(SePiPr_2)_2N\}_2]$

Zn(1)−Se(2)	2.458(9)	Se(2)−Zn(1)−Se(5)	107.31(3)
Zn(1)−Se(5)	2.458(9)	Se(2)−Zn(1)−Se(4)	106.55(3)
Zn(1)−Se(4)	2.459(8)	Se(5)−Zn(1)−Se(4)	114.07(3)
Zn(1)−Se(3)	2.467(9)	Se(2)−Zn(1)−Se(3)	114.07(3)
Se(2)−P(7)	2.177(13)	Se(5)−Zn(1)−Se(3)	106.36(3)
Se(3)−P(6)	2.179(13)	Se(4)−Zn(1)−Se(3)	109.29(3)
Se(4)−P(9)	2.183(13)	P(7)−Se(2)−Zn(1)	103.30(4)
Se(5)−P(8)	2.183(13)	P(6)−Se(3)−Zn(1)	103.01(4)
P(6)−N(10)	1.592(4)	P(9)−Se(4)−Zn(1)	102.83(4)
P(8)−N(11)	1.583(3)	P(8)−Se(5)−Zn(1)	103.67(4)

Table 3. Selected interatomic distances (Å) and angles (°) for $[Zn\{(SPiPr_2)_2N\}_2]$

Zn(1)−S(4)	2.350(11)	S(4)−Zn(1)−S(2)	108.78(4)
Zn(1)−S(2)	2.347(11)	S(4)−Zn(1)−S(1)	106.98(4)
Zn(1)−S(1)	2.351(10)	S(2)−Zn(1)−S(1)	112.81(4)
Zn(1)−S(3)	2.359(11)	S(4)−Zn(1)−S(3)	111.84 (4)
S(1)−P(1)	2.027(13)	S(2)−Zn(1)−S(3)	106.59(4)
S(2)−P(2)	2.032(11)	S(1)−Zn(1)−S(3)	109.92(4)
S(3)−P(3)	2.025(11)	P(1)−S(1)−Zn(1)	105.35(5)
S(4)−P(4)	2.027(12)	P(2)−S(2)−Zn(1)	105.90 (5)
		P(3)−S(3)−Zn(1)	105.81(4)
		P(4)−S(4)−Zn(1)	105.87(4)

the subsequent extension of the P−Se bonds 2.177(13)−2.183(13) Å relative to the free ligand, indicates an increase in delocalization within the architecture due to deprotonation.[19] Crystalline $[Zn\{(SPiPr_2)_2N\}_2]$ as reported by Woollins et al. exhibits completely different unit cell parameters.[18] The unit cell described here contains two independent monomeric molecules versus four reported in the earlier paper.[18]

The zinc atom in $[Zn\{(SePPh_2)_2N\}_2]$ is also coordinated to the selenium atoms through two bidentate ligands forming six-membered chelate rings. The tetrahedral geometry around the zinc atom is distorted which is reflected in the Se−Zn−Se angles which range from 103.85(9) to 115.93(6)° (Table 4). There is no significant difference in the Zn−Se bond lengths of $[Zn\{(SePR_2)_2N\}_2]$ (R = Ph or *i*Pr). The ZnE_2P_2N (E = S or Se) rings have puckered geometries with a distorted boat conformation. This conformation appears to be the most commonly adopted for complexes containing $[R_2P(E)NP(E)R_2]^-$ (E = S or Se) ligands, although other conformations also have been reported with selenium or sulfur and phosphorous atoms at the apices.[29,30]

Table 4. Selected interatomic distances (Å) and angles (°) for $[Zn\{(SePPh_2)_2N\}_2]$

Zn(1)−Se(3)	2.459(3)	Se(3)−Zn(1)−Se(4)	115.93(6)
Zn(1)−Se(4)	2.475(15)	Se(3)−Zn(1)−Se(1)	103.85(9)
Zn(1)−Se(1)	2.482(14)	Se(4)−Zn(1)−Se(1)	111.35(8)
Zn(1)−Se(2)	2.484(19)	Se(3)−Zn(1)−Se(2)	115.03(9)
Se(1)−P(1)	2.171(3)	Se(4)−Zn(1)−Se(2)	106.10(9)
Se(2)−P(2)	2.179(2)	Se(1)−Zn(1)−Se(2)	114.71(5)
Se(3)−P(3)	2.186 (2)	P(1)−Se(1)−Zn(1)	94.11(7)
Se(4)−P(4)	2.187(2)	P(2)−Se(2)−Zn(1)	97.46(7)
		P(3)−Se(3)−Zn(1)	102.22(7)
		P(4)−Se(4)−Zn(1)	94.80(8)

Deposition Studies: In this study, metal chalcogenide thin films have been deposited using air-stable single-source precursors, $[M[(EPiPr_2)_2N\}_2]$ (M = Cd^{II}, Zn^{II} and E = S, Se). The suitability of the precursors were determined by thermogravimetric analysis (TGA) at atmospheric pressure, and all show clean sublimation without any residues, as desirable in precursors for MOCVD studies (Table 5). Deposition of thin films was attempted over a range of substrate temperatures (400 to 500 °C) on glass substrates for one hour with ca. 200 mg of precursor used for each growth experiment.

Table 5. TGA data for compounds **1**−**4**

Compound	T_s (°C)[a]	T_f (°C)[b]
$[Cd\{(SPiPr_2)_2N\}_2]$	237	355
$[Cd\{(SePiPr_2)_2N\}_2]$	310	419
$[Zn\{(SPiPr_2)_2N\}_2]$	222	366
$[Zn\{(SePiPr_2)_2N\}_2]$	240	366

[a] T_s = sublimation temp. [b] T_f = decomposition temp.

Cadmium Sulfide: CdS films were grown from $[Cd\{(SPiPr_2)_2N\}_2]$ at growth temperatures of 425 and 450 °C with a precursor temperature of 250 °C. Deposited films were yellow, transparent and well-adherent to the glass sur-

face. At higher growth temperature (475 °C), slightly dark yellow-brown film was observed after one hour of growth. As-deposited cadmium sulfide films were analysed by XRPD, which indicated that the hexagonal CdS films (Table 6) have been deposited with a preferred orientation along the (002) plane (Figure 4). SEM studies indicate that the morphology of film deposited at 450 °C consists of randomly oriented domains of compacted thin acicular crystallites with ca. 1.75 μm in thickness (Figure 5). Similar morphology was also observed for the film deposited at 425 °C. On the basis of EDAX analyses, the films were found to be slightly cadmium rich with 52%, sulfur (46%) and phosphorous (2%).

Table 6. XRPD data for CdS grown at 425 and 450 °C from $[Cd\{(SPiPr_2)_2N\}_2]$

hkl	JCPDS (06-0314) *d* [Å] (rel. int.)	CdS (425 °C) *d* [Å] (rel. int.)	CdS (450 °C) *d* [Å] (rel. int.)
100	3.58 (75)	3.57 (2)	3.57 (2)
002	3.36 (60)	3.35 (100)	3.36 (100)
101	3.16 (100)	3.14 (5)	3.16 (14)
102	2.45 (25)	2.43 (3)	2.45 (6)
110	2.07 (55)	2.05 (3)	2.06 (2)
103	1.90 (40)	1.89 (17)	1.90 (2)
200	1.79 (18)	N/A	N/A
112	1.76 (45)	1.76 (3)	1.77 (6)

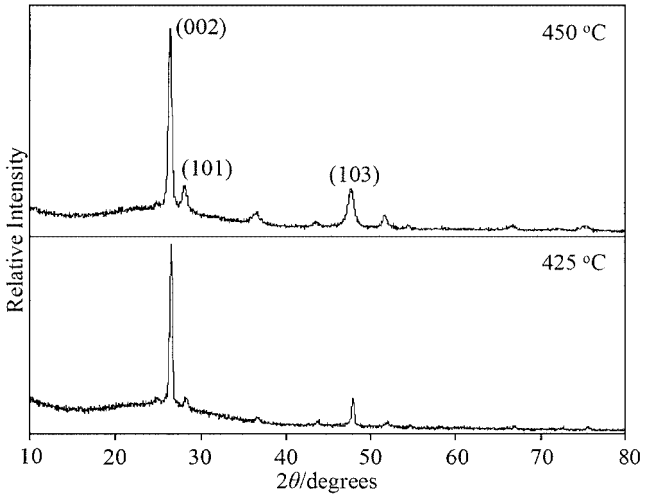

Figure 4. XRPD patterns of CdS films deposited on glass from $[Cd\{(SPiPr_2)_2N\}_2]$ by LP-MOCVD

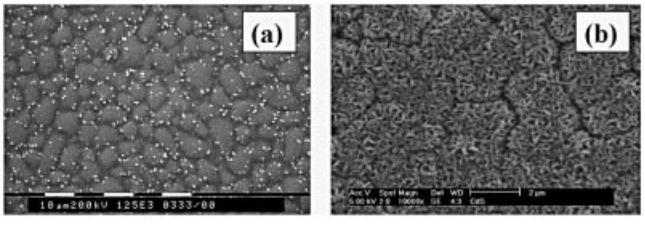

Figure 5. SEM images of CdS films from $[Cd\{(SPiPr_2)_2N\}_2]$ deposited at (a) 425 °C and 450 °C

Cadmium Selenide: Deposition of CdSe films was attempted at substrate temperatures of 425−500 °C, with the precursor temperature set at 325 °C using $[Cd\{(SePiPr_2)_2N\}_2]$. Little or no deposition was observed below 450 °C. At higher growth temperatures, 475 and 500 °C, deposited films were black and adherent to the surface. XRPD studies of the deposited films indicate that polycrystalline hexagonal CdSe films (Table 7) have been deposited with a preferred orientation along the (100) plane (Figure 6). Film deposited at 500 °C was slightly more ordered than the film grown at 475 °C indicated by the absence of (002) plane at 25.5Θ 2θ. Films grown from $[Cd\{(SePPh_2)_2N\}_2]$ also resulted in hexagonal CdSe at 500 and 525 °C but show different preferred orientations (002) and (101) respectively.[17]

Table 7. XRPD data for CdSe grown at 475 and 500 °C from $[Cd\{(SePiPr_2)_2N\}_2]$

hkl	JCPDS (08-0459) *d* [Å] (rel. int.)	CdSe (475 °C) *d* [Å] (rel. int.)	CdSe (500 °C) *d* [Å] (rel. int.)
100	3.72 (100)	3.73 (100)	3.75 (100)
002	3.51 (70)	3.51 (9)	N/A
101	3.29 (75)	3.29 (13)	3.27 (21)
102	2.55 (35)	2.55 (2)	2.54 (1)
110	2.15 (85)	2.15 (36)	2.15 (78)
103	1.98 (70)	1.98 (5)	1.97 (1)
200	1.86 (12)	1.86 (3)	1.86 (8)
112	1.83 (50)	1.83 (7)	1.83 (20)
201	1.80 (12)	1.80 (5)	1.80 (6)
202	1.65 (8)	1.64 (3)	1.64 (3)
203	1.46 (20)	1.45 (6)	1.46 (7)

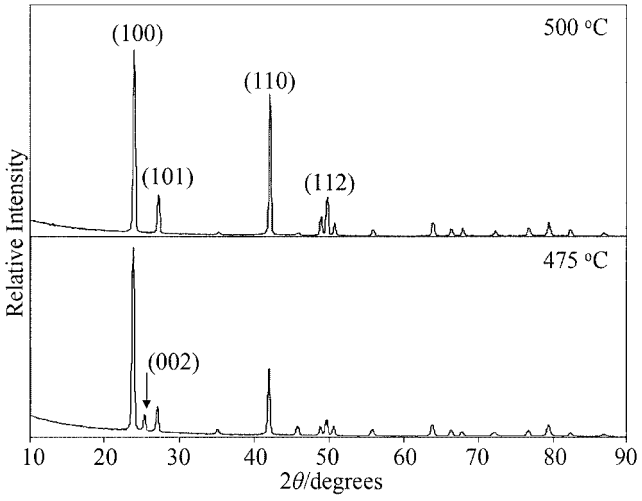

Figure 6. XRPD patterns of CdSe films deposited from $[Cd\{(SePiPr_2)_2N\}_2]$ by LP-MOCVD

SEM studies indicate that the morphology of the film grown at 500 °C consists of randomly orientated platelets (ca. 1 μm in size) (Figure 7b) with a growth rate of ca. 3 μm h^{-1}. At lower growth temperature (475 °C), film morphology consists of clusters of thin particles (Figure 7a). The surface morphology can also be compared with pre-

vious attempts to deposit CdSe films from $[Cd\{(SePPh_2)_2N\}_2]$, which exhibited low degree of crystallinity and growth rate was also significantly lower (1 μm h^{-1}).[17] The EDAX spectrum of the film deposited at 500 °C from $[Cd\{(SeP\textit{i}Pr_2)_2N\}_2]$ shows the presence of cadmium (54%) and selenium (46%). No phosphorous contamination was detected in the films.

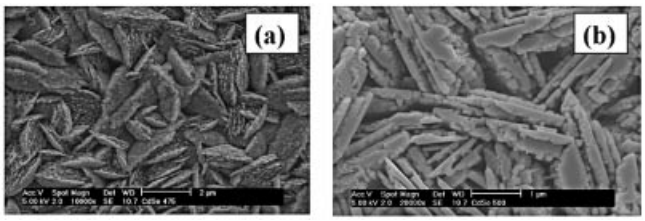

Figure 7. SEM images of CdSe films from $[Cd\{(SeP\textit{i}Pr_2)_2N\}_2]$ deposited at (a) 475 °C and 500 °C

Zinc Sulfide: Non-adherent, brown films were deposited at 450 and 475 °C maintaining precursor temperature at 250 °C using $[Zn\{(SP\textit{i}Pr_2)_2N\}_2]$. Zinc sulfide is known to exist in two phases, at low-temperature cubic polymorph (zinc blende) and at high temperature hexagonal phase (wurtzite).[31] XRPD pattern for the film deposited at 475 °C is shown in (Figure 8) and is consistent with the formation of hexagonal ZnS (JCPDS 36−1450) with a preferred orientation along the (100) plane. At higher growth temperatures (500 °C), deposited film was found to be amorphous indicated by XRPD.

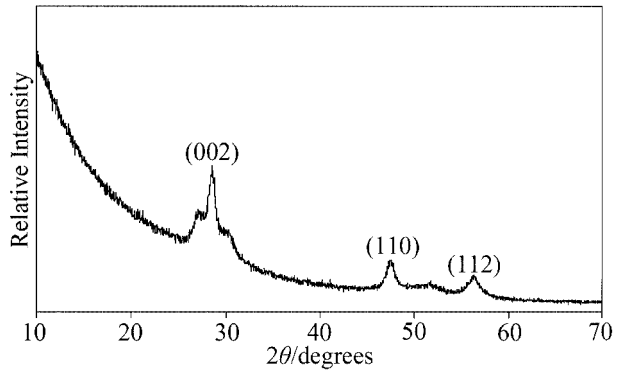

Figure 8. XRPD pattern of ZnS film deposited on glass from $[Zn\{(SP\textit{i}Pr_2)_2N\}_2]$ by LP-MOCVD

SEM micrographs for the film deposited at 475 °C shows that the film surface consists of globules ranging in size 0.25−1.25 μm. Cross-sectional SEM image of the film indicates columnar growth for ZnS and the growth rate is found to be ca. 1 μm h^{-1} (Figure 9). Similar surface morphology also has been observed for the growth of ZnS from previously studied single-source precursors by MOCVD e.g. zinc bis(diisobutyldithiophosphinate)[32] and zinc diethyldithiocarbamate.[33] EDAX indicates the presence of zinc and sulfur, however, 3% of phosphorous was also detected which is incorporated during the decomposition of precursor.

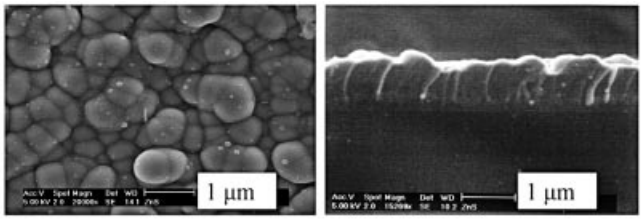

Figure 9. SEM images of ZnS films deposited at 475 °C from $[Zn\{[SP\textit{i}Pr_2)_2N\}_2]$ by LP-MOCVD

Zinc Selenide: ZnSe films were grown over a range of substrate temperatures (400−500 °C) using $[Zn\{(SeP\textit{i}Pr_2)_2N\}_2]$ but the optimum growth temperature appears to be between 425−450 °C with the precursor temperature at 275 °C. As-deposited films were orange-yellow, adherent and specular on the glass substrates. XRPD patterns indicate that the films grown at 425 and 450 °C on glass substrates showed only single-phase hexagonal ZnSe (Table 8, Figure 10). $[Zn\{(SePPh_2)_2N\}_2]$ also deposited hexagonal films at comparatively higher deposition temperatures (500 and 525 °C).[17] At higher growth temperatures

Table 8. XRPD data for ZnSe grown at 425 and 450 °C from $[Zn\{(SeP\textit{i}Pr_2)_2N\}_2]$

hkl	JCPDS (15-0105) *d* [Å] (rel. int.)	ZnSe (450 °C) *d* [Å] (rel. int.)	ZnSe (425 °C) *d* [Å] (rel. int.)
100	3.43 (100)	3.45 (95)	3.45 (100)
002	3.25 (90)	3.28 (69)	3.28 (56)
101	3.05 (70)	3.07 (28)	N/A
102	2.37 (60)	2.38 (5)	N/A
110	2.00 (100)	2.00 (100)	2.00 (70)
103	1.84 (80)	1.85 (7)	N/A
112	1.70 (70)	1.71 (41)	1.71 (25)
202	1.53 (10)	N/A	N/A
203	1.35 (60)	1.36 (2)	N/A

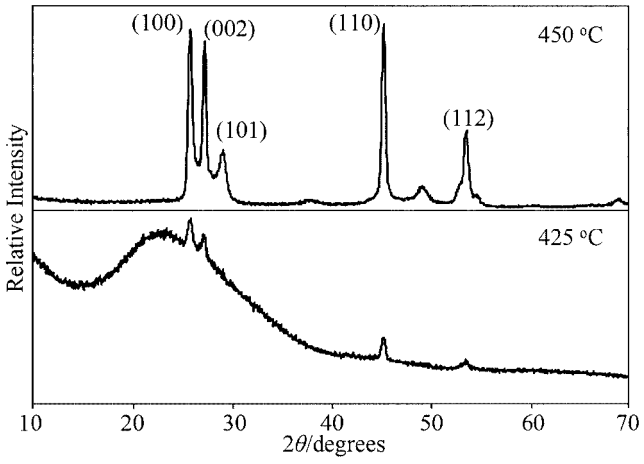

Figure 10. XRPD patterns of ZnSe films deposited from $[Zn\{(SeP\textit{i}Pr_2)_2N\}_2]$ by LP-MOCVD

(450 °C), the crystallinity of deposited film is significantly improved. However, at lower growth temperatures (425 °C), the XRPD pattern was weak indicating a less crystalline film.

SEM micrographs for the film deposited at 450 °C on glass consists of well-defined, randomly orientated particles, with an average size of ca. 0.5 μm (Figure 11). In 1 hour growth, film with ca. 2 μm thickness has been deposited. In contrast, films deposited at 425 °C had platelike morphologies with the plates laid down horizontally with respect to the glass surface. EDAX confirms that the film is close to stoichiometric ZnSe with a small amount of phosphorous (ca. 2%).

The optical properties of the films were measured by UV/Vis spectroscopy. The bandgap values extrapolated for CdS, CdSe, ZnS and ZnSe thin films are 2.30, 1.71, 3.64 and 2.63 eV, respectively. The bandgap values are all close to the literature values of 2.53 (CdS), 1.74 (CdSe), 3.8 (ZnS) and 2.58 eV (ZnSe).[34]

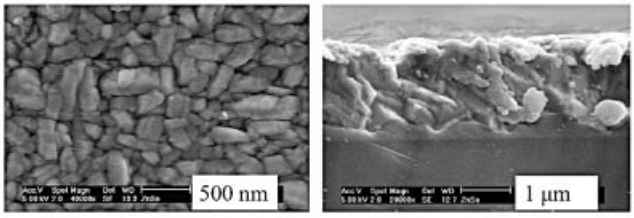

Figure 11. SEM images of ZnSe films deposited at 450 °C from $[Zn\{(SeP\textit{i}Pr_2)_2N\}_2]$ by LP-MOCVD

Conclusion

The air-stable single-source precursors $[M\{(EP\textit{i}Pr_2)_2N\}_2]$ (M = Cd^{II}, Zn^{II} and E = S, Se) have been prepared and characterised by various analytical techniques and utilised as single-source precursors for the deposition of metal chalcogenide thin films by LP-MOCVD. X-ray single crystal structures of zinc compounds indicate distorted tetrahedral geometry at the metal centres. Clean volatilisation of precursors studied by TGA makes them useful for MOCVD studies. XRPD patterns of as-deposited films show that only hexagonal phase of metal sulfide/selenide have been prepared at different growth temperatures.

Experimental Section

Precursor Synthesis: All compounds were prepared by a modified method to that reported in the literature.[18,19] The ligands $[NH(EP\textit{i}Pr_2)_2N]$ (E = S, Se) were sythesised by the reported method.[18,19]

$[Cd\{(SP\textit{i}Pr_2)_2N\}_2]$ (1):[18] In a typical preparation sodium methoxide (1.09 g, 19.7 mmol) was added to a stirred solution of $[NH(SP\textit{i}Pr_2)_2N]$ (6.00 g, 19.2 mmol) in anhydrous methanol (100 cm^3) and stirred for 10 minutes at room temperature. On addition of cadmium chloride (1.76 g, 9.5 mmol) to the resulting solution a white precipitate was formed which was furthur stirred for 2−3 hours, filtered and dried under vacuum. Recrystallisation from dichloromethane/petroleum ether (40−65 °C) yielded 6.2 g (89%) product as white solid. FT-IR: $\tilde{\nu}$ = 1224, 767 (ν P-*N*−P) cm^{-1}. ^1H NMR ($CDCl_3$): δ = 1.3 (m, 48 H, 16 CH_3-R), 2.1 (m, 8 H, 8 R-CH) ppm. ^{31}P NMR ($CDCl_3$): δ = 62.59 ppm. MS (FAB): *m*/*z* = 737 $[M + H^+]$. $C_{24}H_{56}CdN_2P_4S_4$: calcd. C 39.12, H 7.60, N 3.80, P, 16.81; found C 39.30, H 7.80, N 3.74, P 17.11.

$[Cd\{(SeP\textit{i}Pr_2)_2N\}_2]$ (2):[19] Recrystallisation of the white solid product from chloroform/methanol gave white crystals, yield 4.51 g (99%). FT-IR: $\tilde{\nu}$ = 1226, 763 (ν P-*N*−P), 425 (ν P-Se) cm^{-1}. ^1H NMR ($CDCl_3$): δ = 1.15 (m, 48 H, 16 CH_3-R), 2.1 (m, 8 H, 8 R-CH) ppm. ^{31}P NMR ($CDCl_3$): δ = 57.101 ppm. MS (FAB): *m*/*z* = 926 $[M + H^+]$. $C_{24}H_{56}CdN_2P_4Se_4$: calcd. C 31.16, H 6.10, N 3.03, P 13.39; found C 31.33, H 6.15, N 2.98, P 13.53.

$[Zn\{(SP\textit{i}Pr_2)_2N\}_2]$ (3):[18] Recrystallisation from dichloromethane/petroleum ether (40−65 °C) gave a white powder, yield 69%. FT-IR: $\tilde{\nu}$ = 1226, 773 (ν P-*N*−P) cm^{-1}. ^1H NMR ($CDCl_3$): δ = 1.3 (m, 48 H, 16 CH_3-R), 2.1 (m, 8 H, 8 R-CH) ppm. ^{31}P NMR ($CDCl_3$): δ = 63.99 ppm. MS (FAB): *m*/*z* = 689 $[M + H^+]$. $C_{24}H_{56}N_2P_4S_4Zn$: calcd. C 41.79, H 8.55, N 4.06, P 17.96; found C 41.83, H 8.56, N 4.03, P 18.64.

$[Zn\{(SeP\textit{i}Pr_2)_2N\}_2]$ (4):[19] Recrystallisation from chloroform/methanol gave white crystals, yield 4.21 g (98%) white crystals. FT-IR: $\tilde{\nu}$ = 1228, 762 (ν P-*N*−P), 427 (ν P-Se) cm^{-1}. ^1H NMR ($CDCl_3$): δ = 1.2 (m, 48 H, 16 CH_3-R), 2.0 (m, 8 H, 8 R-CH) ppm. ^{31}P NMR ($CDCl_3$): δ = 57.101 ppm. MS (FAB): *m*/*z* = 878 $[M + H^+]$. $C_{24}H_{56}N_2P_4Se_4Zn$: calcd. C 32.83, H 6.43, N 3.19, P 14.11; found C 33.02, H 6.61, N 3.12, P 14.18.

Characterisation Techniques: Unless otherwise stated, all reactions were performed under dry nitrogen using standard Schlenk techniques. All solvents and reagents were purchased from Sigma−Aldrich chemical company and used as received. In addition, toluene was distilled from over sodium under nitrogen. ^1H and ^{31}P NMR studies were carried out with a Bruker AC300 FT NMR Spectrometer. Mass spectra were recorded with a Kratos concept 1S instrument. Infrared spectra were recorded with a Specac single reflectance ATR instrument.

Growth Experiments: Low Pressure Metal-Organic Chemical Vapour Deposition (LP-MOCVD): Thin films of metal chalcogenides were grown on borosilicate glass in a low pressure (≈ 10^{-2} Torr) MOCVD reactor tube which has been described elsewhere.[21] A graphite susceptor holds the substrate dimensions (10 mm × 15 mm) which was heated by a tungsten halogen lamp.

Film Characterisations: X-ray powder diffraction studies were carried out using Philips X'Pert MPD diffractometer by using monochromated Cu-K_α radiation. The samples were mounted flat and scanned from 10° to 90° in a step size of 0.04° with a count rate of 2.5 s. Samples were carbon-coated using Edward's coating system E306A before SEM and EDAX analyses. SEM was carried out by using Philip XL30 FEG and EDAX was preformed with DX4. TGA measurements were carried out by a Seiko SSC/S200 model with a heating rate of 10 °C min^{-1} under nitrogen. Electronic absorption spectra were recorded with Helios-Beta Thermospectronic spectrophotometer.

X-ray Crystallographic Study: Single-crystal X-ray diffraction data for the compounds were collected with a CAD-4 diffractometer and Mo-K_α radiation (λ = 0.71069 Å) using ω-2θ scan. The unit cell parameters were determined by least-squares refinement on diffractometer angles (9.99° ≤ θ ≤ 12.51°) for 25 automatically centred reflections.[22] All data were corrected for absorption by empirical methods (ψ scan)[23] and for Lorentz-polarization effects

by XCAD4.[24] The structures were solved by heavy-atom method using DIRDIF-99[25] programs, refined anisotropically(non-hydrogen atoms) by full-matrix least-squares on F^2 using SHELXL-97[26] program. The H atoms were calculated geometrically and refined with a riding model. In the final stage of refinement data were correct for absorption by DIFABS.[27] The program ORTEP-3[28] was used for drawing the molecules. Crystallographic details and selected interatomic distances and angles are given in Tables 1−4.

CCDC-204283−204285 contain the supplementary crystallographic data for this paper. These data can be obtained free of charge at www.ccdc.cam.ac.uk/conts/retrieving.html [or from the Cambridge Crystallographic Data Centre, 12, Union Road, Cambridge CB2 1EZ, UK; Fax: (internat.) +44-1223/336-033; E-mail: deposit@ccdc.cam.ac.uk].

Acknowledgments

The authors thank the EPSRC, UK for the grants to POB that have made this research possible.

[1] P. O'Brien, in *Inorganic Materials* (Eds.: D. Bruce, D. O'Hare), Wiley, Chichester, **1997**, p. 523.
[2] I. G. Dance, R. G. Garbutt, D. C. Craig, M. L. Scudder, *Inorg. Chem.* **1987**, *26*, 3732−3740.
[3] I. G. Dance, R. G. Garbutt, D. C. Craig, M. L. Scudder, *Inorg. Chem.* **1987**, *26*, 4057−4064.
[4] I. G. Dance, R. G. Garbutt, M. L. Scudder, *Inorg. Chem.* **1990**, *29*, 1571−1577.
[5] M. B. Hursthouse, O. F. Z. Khan, M. Mazid, M. Motevalli, P. O'Brien, *Polyhedron* **1990**, *9*, 541−544.
[6] O. F. Z. Khan, P. O'Brien, *Polyhedron* **1991**, *10*, 325−332.
[7] M. Bochmann, K. J. Webb, M. Harman, M. B. Hursthouse, *Angew. Chem. Int. Ed. Engl.* **1990**, *29*, 638−639.
[8] M. Bochmann, K. J. Webb, M. B. Hursthouse, M. Mazid, *J. Chem. Soc., Dalton Trans.* **1991**, 2317−2323.
[9] M. Bochmann, K. J. Webb, *J. Chem. Soc., Dalton Trans.* **1991**, 2325−2329.
[10] B. O. Dabbousi, P. J. Bonasia, J. Arnold, *J. Am. Chem. Soc.* **1991**, *113*, 3186−3188.
[11] P. J. Bonasia, J. Arnold, *Inorg. Chem.* **1992**, *31*, 2508−2514.
[12] C. Byrom, M. A. Malik, P. O'Brien, A. J. P. White, D. J. Williams, *Polyhedron* **2000**, *19*, 211−215.
[13] R. Nomura, T. Murai, T. Toyosaki, H. Matsuda, *Thin Solid Films* **1995**, *271*, 4−7.
[14] M. B. Hurthouse, M. A. Malik, M. Motevalli, P. O'Brien, *Polyhedron* **1992**, *11*, 45−48.
[15] M. Motevalli, P. O'Brien, J. R. Walsh, I. M. Watson, *Polyhedron* **1996**, *15*, 2801−2808.
[16] M. Chunggaze, M. A. Malik, P. O'Brien, *J. Mater. Chem.* **1999**, *10*, 2433−2437.
[17] M. Afzaal, S. M. Aucott, D. Crouch, P. O'Brien, J.-H. Park, J. D. Woollins, *Adv. Mater. Chem. Vap. Dep.* **2002**, *5*, 187−189.
[18] D. Cupertino, R. Keyte, A. M. Z. Slawin, D. J. Williams, J. D. Woollins, *Inorg. Chem.* **1996**, *35*, 2695−2697.
[19] D. Cupertino, D. J. Birdsall, A. M. Z. Slawin, J. D. Woollins, *Inorg. Chim. Acta* **1999**, *290*, 1−7.
[20] V. Garcia-Montalvo, J. Novosad, P. Kilian, J. D. Woollins, A. M. Z. Slawin, P. G. Y. Garcia, M. Lopez-Cardoso, G. Espinosa-Perez, R. Cea-Olivares, *J. Chem. Soc., Dalton Trans.* **1997**, 1025−1029.
[21] M. A. Malik, P. O'Brien, *Adv. Mater. Opt. Electron* **1994**, *7*, 117−121.
[22] Enraf−Nonius CAD-4/PC Software. Version 1.5c, Enraf−Nonius, Delft, The Netherlands, **1994**.
[23] A. C. T. North, D. C. Phillips, F. S. Mathews, *Acta Crystallogr., Sect. A* **1968**, A24, 351−359.
[24] Harms, S. Wocadlo, *XCAD4 − CAD4 Data Reduction*, University of Marburg, Marburg. Germany, **1995**.
[25] P. T. Beurskens, G. Beursken, W. Bosman, R. De Gelder, S. Garci-Granda, R. O. Gould, R. Israel, J. M. M. Smiths, *The DIRDIF-96 Programme system*, Crystallography Laboratory, University of Nijmegen, The Netherlands, **1996**.
[26] G. Sheldrick, M. SHELXL-97, University of Göttingen, **1997**.
[27] L. J. Farrugia, ORTEP-3 for Windows, *J. Appl. Crystallogr.* **1997**, *30*, 565.
[28] L. J. Farrugia, *WinGX − A Windows Program for Crystal Structure Analysis*, University of Glasgow, Glasgow, **1998**.
[29] J. R. Philips, A. M. Z. Slawin, A. J. P. White, D. J. Williams, J. D. Woollins, *J. Chem. Soc., Dalton Trans.* **1995**, 2467−2468.
[30] N. Zuniga-Villarreal, C. Silvestru, R. R. Lezama, S. H. Ortega, C. A. Toledano, *J. Organomet. Chem.* **1995**, *496*, 169−174.
[31] P. O'Brien, R. Nomura, *J. Mater. Chem.* **1995**, *5*, 1761−1773.
[32] Y. Takahashi, R. Yuki, M. Sugiura, S. Motijima, K. Sugiiyama, *J. Cryst. Growth* **1980**, *50*, 491−497.
[33] N. H. Tran, R. N. Lamb, G. L. Mar, *Colloids Surfaces A., Physicochem. Eng. Aspects* **1999**, *155*, 93−100.
[34] J. I. Pankove, *Optical processes in semiconductors*, Dover Publications Inc., New York, **1970**, 1327.

Received February 19, 2003
Early View Article
Published Online October 23, 2003

